

Received December 30, 2019, accepted January 16, 2020, date of publication January 22, 2020, date of current version January 31, 2020.

Digital Object Identifier 10.1109/ACCESS.2020.2968619

A Novel Snowflake Fractal Antenna for Dual-Beam Applications in 28 GHz Band

HIDAYAT ULLAH¹ AND FAROOQ A. TAHIR¹ , (Senior Member, IEEE)

Research Institute for Microwave and Millimeter-Wave Studies, National University of Sciences and Technology, Islamabad 44000, Pakistan

Corresponding author: Farooq A. Tahir (farooq.tahir@seecs.edu.pk)


This work was financially supported in part by Higher Education Commission (HEC) of Pakistan through its National Research Program for Universities (NRPU) under Project 10070/Federal/NRPU/R&D/HEC/2017.

ABSTRACT A wideband snowflake antenna for 28 GHz millimeter-wave communications is proposed. The antenna has a size of $8 \times 5 \text{ mm}^2$, fabricated on ultra-thin 0.254 mm substrate. The antenna consists of four small hexagons surrounding a bigger hexagon in order to attain broadband characteristics. Bandwidth response of the antenna is between 25.28–29.04 GHz (13.43% @ 28 GHz), having 3.12 dBi gain and more than 80% of radiation as well as total efficiency. The antenna specific structure is designed such that it gives dual beam over its entire bandwidth without a noticeable shift in its beam directions. For enhanced gain performance, its 4-element array (of size $32 \times 12 \text{ mm}^2$) has been fabricated separately to increase its gain upto 10.12 dBi at 28 GHz. The proposed dual-beam antenna and its array has been modelled on thin Rogers substrate to show that its application in millimeter-wave communication equipment is viable.

INDEX TERMS 5G, millimeter-wave, 28 GHz, broadband, dual-beam antennas, arrays, smartphones.

I. INTRODUCTION

The evolution of mobile communication systems is undergoing through a stage where there is a need for supreme data-rates in the range of giga-bits-per-second. This enormous need for high speed is challenging for researchers and the solution that has surfaced consequently, is to upgrade physical communication in millimeter-wave spectrum above 6 GHz. The already choking spectrum has thus to be left behind and a new unlimited bandwidth available at millimeter-wave range has to be harnessed [1]. Feasibility studies have been carried out in order to see whether this high frequency range is capable of delivering the required speeds or not. The experimental results show that millimeter-wave communication above 6 GHz is not only a mere possibility but is suitable for becoming a standard for future [2]. Frequency bands have been allocated for millimeter-wave communications which includes unlicensed bands for example the 57–64 GHz (O_2 band), 164–200 GHz (H_2O band) [3] and licensed bands such as 28 GHz and 38 GHz bands [4]. The unlicensed bands have however very high attenuation per kilometer. To operate in these bands, the antennas are desirable to have high gains and large bandwidth [5].

The associate editor coordinating the review of this manuscript and approving it for publication was Hassan Tariq Chattha .

Recently, quite a large number of antennas are being designed and published by the research community that target operation in the millimeter-wave spectrum [6]–[14]. Their structures vary according to working mechanism, fabrication complexities and cost. For example, the 28 GHz antenna by Park [6] is structured in multiple layers that is fed through a substrate-integrated-waveguide. The antenna through its low-side-lobe levels attains a peak gain of 13.97 dBi. This antenna however is complex due to the use of waveguide-to-SIW transition and asymmetric via posts inside SIW feed. The antenna by Choubey [7] for 28 and 45 GHz bands provides large bandwidth but at the cost of increased complexity in its structural design. Similarly, a very complex design [8] by Dadgarpour using multi-layered metamaterial structure provides 15 dBi gain. On the other hand, simple planar antennas of comparable performances are preferable because of their low fabrication costs. The antenna by Khalily [9] for example has 15.6 dBi gain bearing an overall size of $20 \times 20 \text{ mm}^2$ and those of [10], [11] have large bandwidths of around 10 GHz.

The antennas working in the unlicensed bands [12]–[14] are not preferable because of high absorption characteristics of the operational bands for example the O_2 and H_2O bands. In order to increase the reliability of communications in these bands, antennas must be made robust to cater for the losses

TABLE 1. Optimized parameters of the antenna.

Parameter	Value (mm)
a	0.49
b	0.55
R	0.8
h	0.4
w	0.4
W_s	8
L_s	5
W_f	0.8
L_f	2.2
L_g	2

incurred. For example, the circular polarization [12] and dual-beam [13] nature of these antennas can make them more suitable for challenging channel propagation characteristics. Similarly, SIW cavity used in [14] enables the antenna to get an extremely high gain of 26.7 dBi to make it usable in these unlicensed absorptions bands.

The dual-beam antennas are especially attractive in that they can be used for spatial diversity applications [15]. These antennas are used for scenarios where adjacent channels interference effects need minimization [16]. Several dual-beam antennas have been the focus of millimeter-wave designs such as [8] and [17], [18]. These antennas are however complex by design due to the multi-structure nature [17] and metamaterial design methodology [8], [18]. Instead, simple and planar structural designs can also acquire similar performances such as high gain and large bandwidth [19]–[22].

We have proposed a simple planar antenna based on a thin substrate that gives a dual-beam performance over a wide bandwidth. Dual-beam pattern remains stable over the desired frequency range due to the inherent symmetric geometry of the antenna. Furthermore, in order to get a high gain, a 4-element array of the same dual-beam antenna has been constructed.

II. ANTENNA DESIGN

A. DUAL BEAM ANTENNA DESIGN

The dual-beam antenna is built upon a 0.254 mm thick Rogers RT/Duroid 5880 ($\epsilon_r = 2.2$, $\tan\delta = 0.0009$) substrate. The dual-beam antenna is $8 \times 5 \text{ mm}^2$ and its structure is shown in Fig. 1. Its optimized parameters are given in Table 1.

The dual-beam antenna top side consists of a two-stage fractal design. The back side consists of a standard truncated ground with a central block-notch. The antenna consists of a central hexagon of radius ‘R’ and is fed by a microstrip line. The hexagon and microstrip line combined together constitute basic set of the design. Each corner of this central hexagon is then further connected to another set of a microstrip line and a hexagon pair of smaller dimensions ‘a’ and ‘b’. The overall dual-beam antenna structure is therefore a two-stage fractal design, which has a generator block consisting of a microstrip line and hexagon. The final structure resembles a snowflake, which consists of a big central

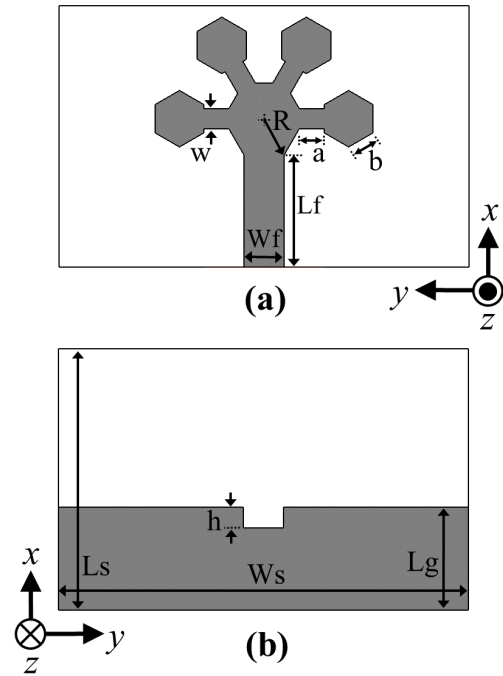


FIGURE 1. Geometry of the proposed antenna (a) front view (b) back view.

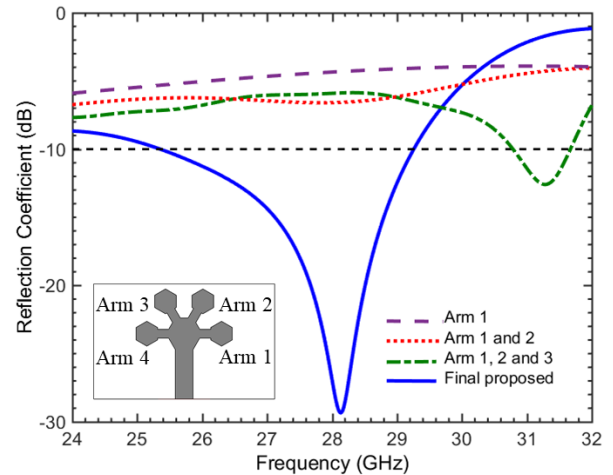


FIGURE 2. Simulated reflection coefficient (S11) showing the effect of number of arms of the dual-beam antenna.

hexagon having four smaller hexagonal arms. The effect of number of arms over impedance matching of the dual-beam antenna is illustrated in Fig. 2. It can be seen that as the number of arms is increased from 1 to 4, impedance of the dual-beam antenna gets matched in a better way.

Resonant frequency of the dual-beam antenna can be fully controlled by varying parameters ‘R’, ‘a’ and ‘b’. The target band is 28 GHz millimetre-wave band. The first parametric analysis is given in Fig. 3, which shows response of the antenna to change in radius of the central hexagon. It is observed that parameter ‘R’ plays a pivotal role in adjusting resonance of the dual-beam antenna.

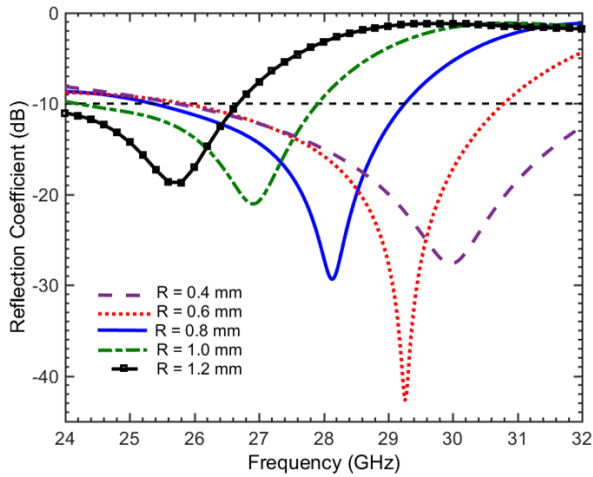


FIGURE 3. Effect of radius of the central hexagon over S11.

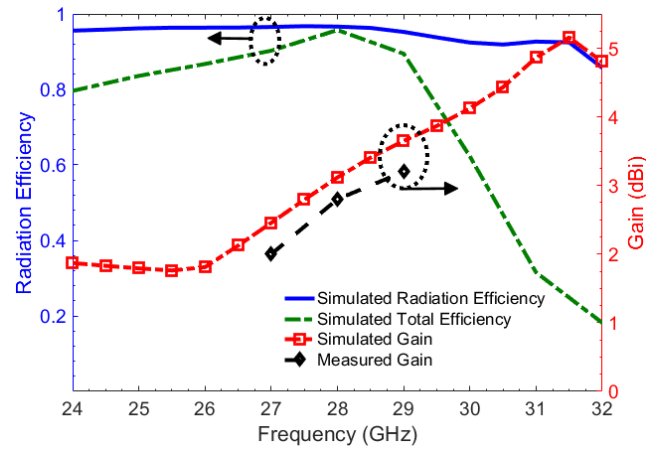


FIGURE 5. Radiation, total efficiencies, simulated and measured gain of the dual-beam antenna.

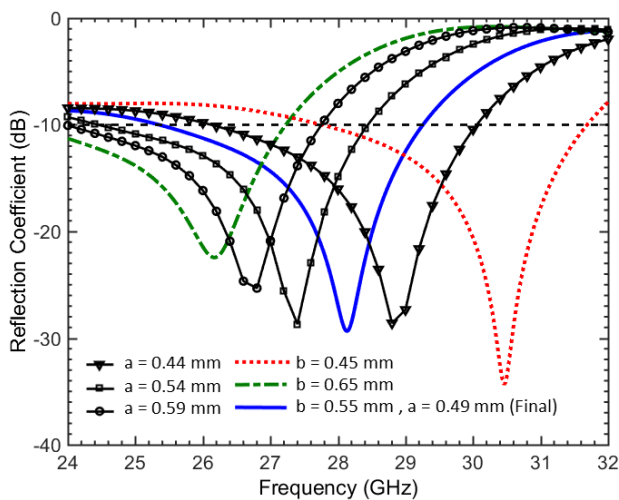


FIGURE 4. Effect of smaller hexagon and extension arm over the reflection coefficient of the single element.

The antenna can further be optimized by parameters ‘a’ and ‘b’ whose effect is shown in Fig. 4. It can be observed that reflection coefficient of the dual-beam antenna is quite sensitive to changes in size of the smaller hexagons. In conjunction with this, the length ‘a’ of extension arm can be used to get even more flexibility in adjusting resonance.

The radiation and total efficiency along with simulated and measured gain of the dual-beam antenna is given in Fig. 5. The antenna is more than 80 % efficient in its operating band. This is primarily due to the fact that the substrate used for this design has a very low loss with $\tan\delta = 0.0009$. Gain of the antenna is between 1.78-3.76 dBi considering its operating range. At 28 GHz, the gain is 3.12 dBi which is an appreciable value for any dual beam antenna.

The surface current distribution is given in Fig. 6. Structure of the dual-beam antenna design is symmetric. There are four small hexagons which are placed at an angle of 60° around the central hexagon. The resultant current distribution

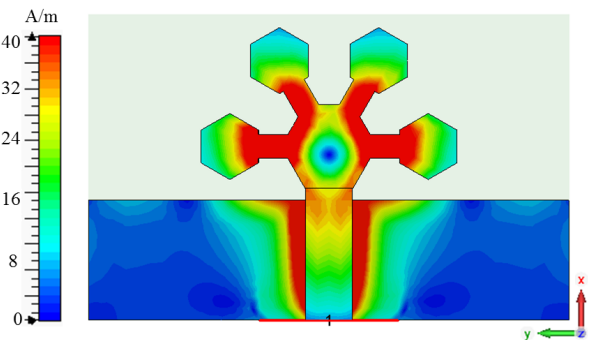


FIGURE 6. Surface current distribution of the dual beam antenna at 28 GHz.

is therefore symmetric in nature as well. It can be easily observed that the left and right hand side of antenna current distributions are mirror images of each other. The design objective is to acquire symmetric dual-beam characteristics from this antenna. Normalized radiation pattern of the dual-beam antenna is depicted in Fig. 7 at various frequencies. It is verified that the antenna indeed possesses two distinct beams symmetrically located on either side of its center. In xy-plane (i.e. $\theta = 90^\circ$ plane), at 28 GHz there are main beams at $\varphi = -50^\circ$ and $\varphi = +50^\circ$ respectively with beam-width of 58° .

For an unsymmetrical structure, the radiation pattern variation is such that it become undesirable for fixed beam applications. The radiation pattern graphs of Fig. 7 also shows that these dual-beams remain fixed at $\pm 50^\circ$ over the entire operational bandwidth. This has been made possible due to the designed symmetric structure of the dual-beam antenna. The 3dB power beam width analysis reveals that the HPBW is inversely proportional to frequency. The two beams are separated by a strong null at 0° in the xy-plane.

It should be noted that the physical angle between the top two fractal arms of the dual-beam antenna is 60° , which results in two beams that are approximately at 50° from the x-axis. If the physical angle between these two fractal arms is changed, the direction of radiated beams will also change. Furthermore, beam-width of any of the beams is

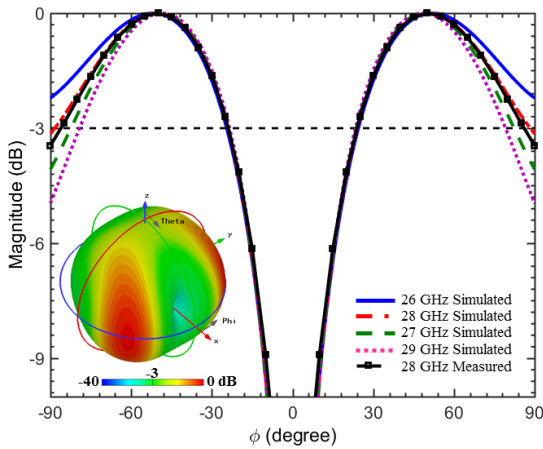


FIGURE 7. Radiation patterns at 26, 27, 28 and 29 GHz in $\theta = 90^\circ$ plane (xy-plane). Inset shows normalized 3D gain @ 28 GHz.

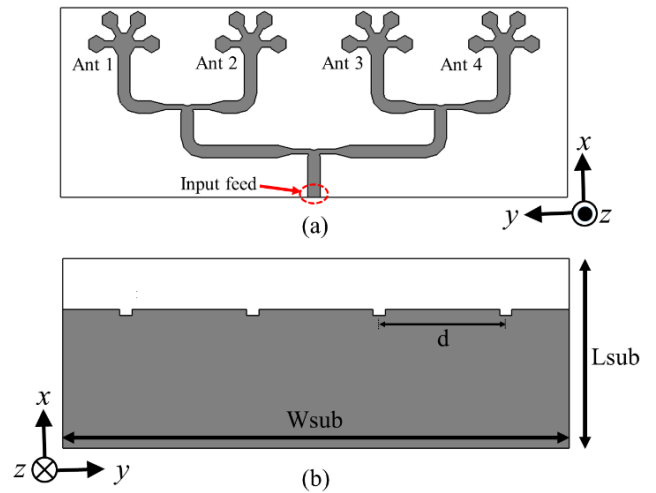


FIGURE 9. Structure of the antenna array (a) front side (b) back side.

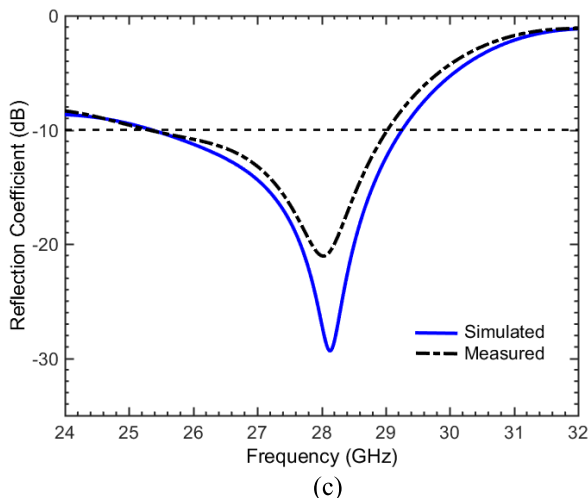
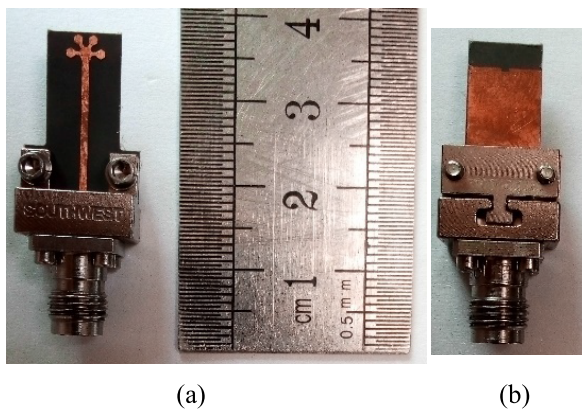


FIGURE 8. Photograph of the fabricated dual beam antenna (a) front side (b) back side (c) simulated and measured reflection coefficient.

approximately 58° , which also corresponds to the separation angle between the side fractal arms. By changing this separation angle, we will be able to change the beam-width of the beams. Therefore, we have two degrees of freedom in this particular snowflake design. First, we can control the beam direction w.r.t. x-axis and secondly, we can change beam-width of the beams. This controllability is achieved by simply

changing the physical angle between fractal arms of the dual-beam antenna.

III. FABRICATION AND MEASUREMENT

The dual-beam antenna as well a 4-element array antenna was fabricated using a standard PCB process using a Rogers RT/Duroid 5880 substrate. A Southwest 2.4 mm RF connector was used to feed the antenna. The fabricated dual-beam antenna is shown in Fig. 8 (a) (b) along with its simulated and measured reflection coefficient graph. The measured impedance bandwidth of dual-beam antenna is in the range 25.28 – 29.04 GHz that is 3.76 GHz of bandwidth (i.e. 13.43% @ 28 GHz). It should be noted here that the feed line has been extended by 10 mm in order to minimize the effect of RF connector in close proximity. The dual-beam antenna measured radiation pattern at 28 GHz, as shown in Fig. 7, indicate that good agreement exists with the anticipated dual-beam radiation pattern.

IV. ARRAY CONFIGURATION

As an additional step, we have constructed a 4-element array from our proposed dual-beam antenna. This has been done to enhance the antenna gain from around 3.12 dBi at 28 GHz to as high as 10.15 dBi at 28 GHz. A special microstrip feed network designed for 28 GHz with low loss and compact size has been used. The feed network proposed by [19] has been used to excite an array of 4-elements of the proposed antenna. This feed network has been constructed using microstrip line, T-junction and 90° -bend to input in-phase and equal magnitude waveform to the antenna elements. The element spacing, however, has been kept to $d = 8$ mm which corresponds to $0.72\lambda_0$ at 28 GHz. This separation ensures broadside pattern with two beams (along $\theta = 0^\circ, 180^\circ$). The 2nd beam is a grating lobe formed at 28 GHz. This feed network has low radiation losses due to its efficient design and has reflection coefficient magnitude that is less than -15 dB throughout a wide operating frequency (24-35 GHz) range.

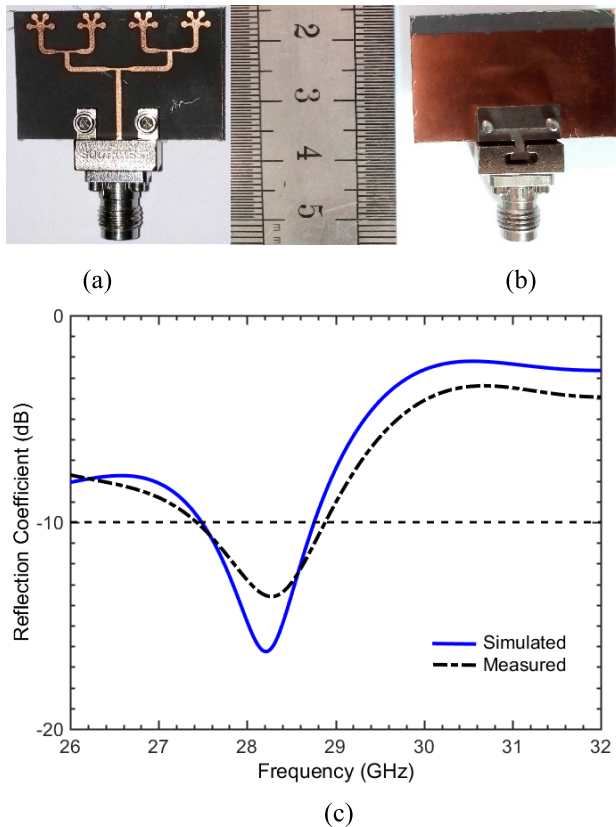


FIGURE 10. Photograph of the fabricated antenna array (a) front side (b) back side (c) simulated and measured reflection coefficient.

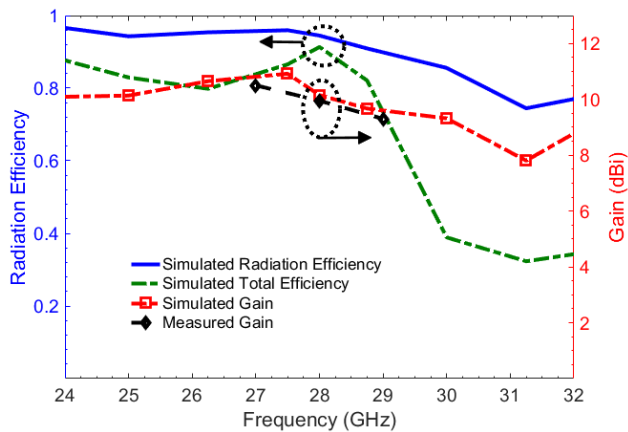


FIGURE 11. Radiation, total efficiencies, simulated and measured gain of the antenna array.

The feed network combined with 4-elements of the dual-beam antenna forms a complete antenna array. This antenna array is shown in Fig. 9. The antenna array overall size is $L_{sub} = 12$ mm and $W_{sub} = 32$ mm.

The antenna array was also fabricated using the same technique and is shown in Fig. 10 (a) (b). Reflection coefficient S11 of the array antenna is shown in Fig. 10(c). It can be seen here that the antenna array resonates at the same frequency i.e. 28 GHz as that of the dual-beam antenna. However, the bandwidth has reduced to 27.45-28.86 GHz which is 1.41 GHz (i.e. 5.03% @ 28 GHz). The antenna array gain

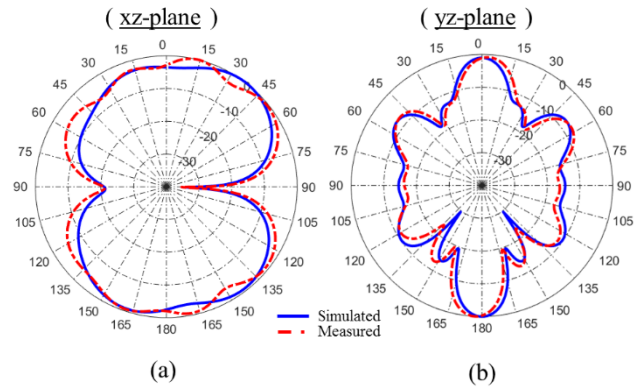


FIGURE 12. Normalized radiation pattern of the antenna array at 28 GHz in (a) xz-plane (b) yz-plane.

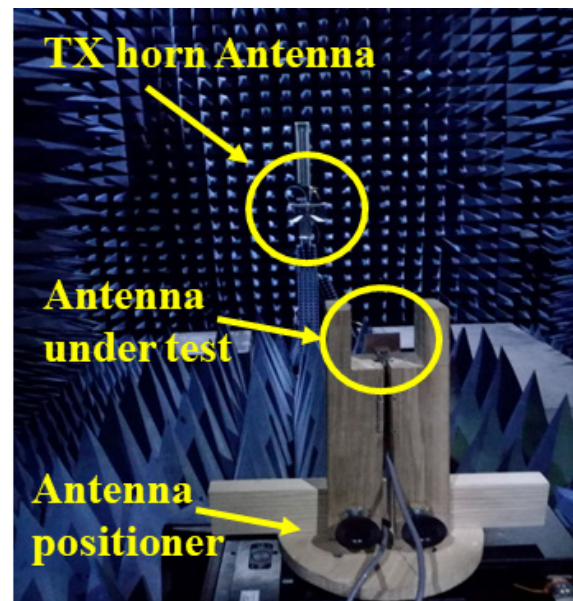


FIGURE 13. Photograph of the antenna array during measurement inside in an anechoic chamber.

and efficiency plots are depicted in Fig. 11. The array gain varies between 7.8-10.9 dBi with a value of 10.15 dBi at 28 GHz. The radiation and total efficiency is well above 80% in operational band of the antenna.

Normalized radiation patterns of the antenna array at 28 GHz is shown in Fig. 12. The pattern in xz-plane indicate that it radiates in all directions with exception of two nulls, located towards top and bottom side of the antenna array. The yz-plan pattern indicate that the antenna is directive and there are radiations towards front and bottom side of the antenna. Simulated beam-width of the antenna is 18.2° in yz-plan, which is suitable for millimeter-wave communications in future mobile network. The measured results are in good agreement with those simulated. Measurements were performed at in-house facility, and photograph of the setup is shown in Fig. 13.

The formation of array antenna from original dual-beam antenna has brought an addition of approximately 7 dBi gain at 28 GHz. This value of gain is very useful for millimeter wave communication, where high gain is a key requirement

for long distance communication. However, dual-beam of the original antenna, that were directed at $\pm 50^\circ$ w.r.t x-axis have been replaced by two beams that are at 180° with respect to each other. These two beams can be seen in Fig. 12 (b), where there is a main lobe at 0° and a back lobe at 180° . The back lobe (i.e. grating lobe) acts as our 2nd beam. Here we must notice that the direction of these beams however cannot be changed through minor modifications in the fractal arms, and hence will remain fixed at 0° and 180° .

V. CONCLUSION

A dual-beam broadband antenna having 3.76 GHz of bandwidth in the 28 GHz millimeter-wave band has been modelled and analyzed. The antenna possesses a unique structural layout based on fractals, which gives an overall broadband performance. The antenna has been designed specifically in such a manner that it possess dual-beam at $\pm 50^\circ$ in its xy-plane. These two beams remains fixed at their respective locations even if there is a change in the operating frequency. The dual-beam characteristics of this antenna will find its application in spatial diversity techniques. Furthermore, an array of 4-elements has also been fabricated for high gain millimeter-wave communication. The array antenna has 10.12 dBi gain at 28 GHz. The antenna array has two beams point at 180° with respect to each other. The antenna possess an extremely small size ($8 \times 5 \text{ mm}^2$ dual-beam antenna and $32 \times 12 \text{ mm}^2$ for array) suitable for integration into to hand-held devices. The proposed antenna has excellent features which will prove useful for its application in high speed communication in the millimeter-wave spectrum.

REFERENCES

- [1] Y. Wang, J. Li, L. Huang, Y. Jing, A. Georgakopoulos, and P. Demestichas, "5G mobile: Spectrum broadening to higher-frequency bands to support high data rates," *IEEE Veh. Technol. Mag.*, vol. 9, no. 3, pp. 39–46, Sep. 2014.
- [2] W. Roh, J.-Y. Seol, J. Park, B. Lee, J. Lee, Y. Kim, J. Cho, K. Cheun, and F. Aryanfar, "Millimeter-wave beamforming as an enabling technology for 5G cellular communications: Theoretical feasibility and prototype results," *IEEE Commun. Mag.*, vol. 52, no. 2, pp. 106–113, Feb. 2014.
- [3] Z. Pi and F. Khan, "An introduction to millimeter-wave mobile broadband systems," *IEEE Commun. Mag.*, vol. 49, no. 6, pp. 101–107, Jun. 2011.
- [4] (Aug. 2015). *5G Spectrum Recommendations*. [Online]. Available: <http://www.5gamericas.org>
- [5] C. Dehos, J. L. González, A. D. Domenico, D. Ktenas, and L. Dussopt, "Millimeter-wave access and backhauling: The solution to the exponential data traffic increase in 5G mobile communications systems?" *IEEE Commun. Mag.*, vol. 52, no. 9, pp. 88–95, Sep. 2014.
- [6] S.-J. Park, D.-H. Shin, and S.-O. Park, "Low side-lobe substrate-integrated-waveguide antenna array using broadband unequal feeding network for millimeter-wave handset device," *IEEE Trans. Antennas Propag.*, vol. 64, no. 3, pp. 923–932, Mar. 2016.
- [7] P. N. Choubey, W. Hong, Z.-C. Hao, P. Chen, T.-V. Duong, and J. Mei, "A wideband dual-mode SIW cavity-backed triangular-complementary-split-ring-slot (TCSRS) antenna," *IEEE Trans. Antennas Propag.*, vol. 64, no. 6, pp. 2541–2545, Jun. 2016.
- [8] A. Dadgarpour, M. Sharifi Sorkherizi, and A. A. Kishk, "Wideband low-loss magnetolectric dipole antenna for 5G wireless network with gain enhancement using meta lens and gap waveguide technology feeding," *IEEE Trans. Antennas Propag.*, vol. 64, no. 12, pp. 5094–5101, Dec. 2016.
- [9] M. Khalily, R. Tafazolli, T. A. Rahman, and M. R. Kamarudin, "Design of phased arrays of series-fed patch antennas with reduced number of the controllers for 28-GHz mm-wave applications," *IEEE Antennas Wireless Propag. Lett.*, vol. 15, pp. 1305–1308, 2016.
- [10] S. X. Ta, H. Choo, and I. Park, "Broadband printed-dipole antenna and its arrays for 5G applications," *IEEE Antennas Wireless Propag. Lett.*, vol. 16, pp. 2183–2186, 2017.
- [11] Q.-X. Chu, X.-R. Li, and M. Ye, "High-gain printed log-periodic dipole array antenna with parasitic cell for 5G communication," *IEEE Trans. Antennas Propag.*, vol. 65, no. 12, pp. 6338–6344, Dec. 2017.
- [12] D. J. Bisharat, S. Liao, and Q. Xue, "High gain and low cost differentially fed circularly polarized planar aperture antenna for broadband millimeter-wave applications," *IEEE Trans. Antennas Propag.*, vol. 64, no. 1, pp. 33–42, Jan. 2016.
- [13] A. Dadgarpour, B. Zarghoomi, B. S. Virdee, and T. A. Denidni, "Single end-fire antenna for dual-beam and broad beamwidth operation at 60 GHz by artificially modifying the permittivity of the antenna substrate," *IEEE Trans. Antennas Propag.*, vol. 64, no. 9, pp. 4068–4073, Sep. 2016.
- [14] Q. Zhu, K. B. Ng, C. H. Chan, and K.-M. Luk, "Substrate-integrated-waveguide-fed array antenna covering 57–71 GHz band for 5G applications," *IEEE Trans. Antennas Propag.*, vol. 65, no. 12, pp. 6298–6306, Dec. 2017.
- [15] S. Kirthiga and M. Jayakumar, "Performance of dualbeam MIMO for millimeter wave indoor communication systems," *Wireless Pers Commun.*, vol. 77, no. 1, pp. 289–307, Jul. 2014.
- [16] K. Hosoya, N. Prasad, K. Ramachandran, N. Orihashi, S. Kishimoto, S. Rangarajan, and K. Maruhashi, "Multiple sector ID capture (MIDC): A novel beamforming technique for 60-GHz band multi-Gbps WLAN/PAN systems," *IEEE Trans. Antennas Propag.*, vol. 63, no. 1, pp. 81–96, Jan. 2015.
- [17] A. Dadgarpour, M. S. Sorkherizi, and T. A. Denidni, "Passive beam switching and dual-beam radiation slot antenna loaded with ENZ medium and excited through ridge gap waveguide at millimeter-waves," *IEEE Trans. Antennas Propag.*, vol. 102, no. 1, pp. 92–102, Nov. 2017.
- [18] J. Tan, W. Jiang, S. Gong, T. Cheng, J. Ren, and K. Zhang, "Design of a dual-beam cavity-backed patch antenna for future fifth generation wireless networks," *IET Microw., Antennas Propag.*, vol. 12, no. 10, pp. 1700–1703, Aug. 2018.
- [19] H. Ullah and F. A. Tahir, "A broadband wire hexagon antenna array for future 5G communications in 28 GHz band," *Microw. Opt. Technol. Lett.*, vol. 61, no. 3, pp. 696–701, Mar. 2019.
- [20] H. Ullah and F. A. Tahir, "Broadband planar antenna array for future 5G communication standards," *IET Microw., Antennas Propag.*, vol. 13, no. 15, pp. 2661–2668, 2019.
- [21] H. Ullah, F. A. Tahir, and M. U. Khan, "A honeycomb-shaped planar monopole antenna for broadband millimeter-wave applications," in *Proc. 11th Eur. Conf. Antennas Propag. (EUCAP)*, Paris, France, 2017, pp. 3094–3097.
- [22] H. Ullah, F. A. Tahir, and M. U. Khan, "Dual-band planar spiral monopole antenna for 28/38 GHz frequency bands," in *Proc. IEEE Int. Symp. Antennas Propag. USNC/URSI Nat. Radio Sci. Meeting*, San Diego, CA, USA, 2017, pp. 761–762.



HIDAYAT ULLAH received the bachelor's degree (Hons.) in electrical engineering from the University of Engineering and Technology (UET) Peshawar, Pakistan, in 2001, and the master's degree (Hons.) in communications engineering from the University of Birmingham, U.K., in 2005. He is currently pursuing the Ph.D. degree in electrical engineering with the National University of Sciences and Technology (NUST), Islamabad. He worked as a Research Engineer with Career

Telephone Industries (Pvt) Ltd., Islamabad, from 2002 to 2004, on a multichannel digital radio (MCDR) system for rural areas. He worked as a Knowledge Transfer Partnership (KTP) Associate on a vehicular communication research project partnership between Loughborough University and JCB England, from 2006 to 2008. The project was sponsored by the Department of Trade and Industries (DTI) U.K. He was placed at JCB World Headquarter, Rocester Staffordshire. He served as the Manager with Space and Upper Atmosphere Research Commission (SUPARCO), Lahore on Paksat-1R Satellite project, from 2009 to 2011. He served as the Assistant Professor in a private university in Peshawar, from 2012 to 2015. He is also active in his research on 5G and millimeter wave antennas.



FAROOQ A. TAHIR (Senior Member, IEEE) received the bachelor's degree in electrical engineering from the University of Engineering and Technology, Lahore, Pakistan, in 2005, the M.S. degree in RF telecommunications and microelectronics (TRFM) from the University of Nice, Sophia Antipolis, France, in 2008, and the Ph.D. degree from the leading French Research Lab LAAS-CNRS Toulouse, France, under the Research Group Micro and Nano Systems for Wireless Communications, in 2011. During Ph.D., his research was focused on the electromagnetic modeling of electronically reconfigurable reflectarrays

for LEO satellites in x-band. This Research was carried out under a Joint Research Project of European Space Agency (ESA), Thales Alenia Space, and French Research Agency. His Ph.D. Thesis was nominated for Best Thesis Prize of 2011 with the National Polytechnique Institute of Toulouse, France. He has also been involved in the project entitled *RF MEMS-Based Reconfigurable Reflectarray Antenna* (R3MEMS) funded by French Research Agency and Thales Alenia Space. He is currently serving as an Associate Professor with the National University of Sciences and Technology, Islamabad, Pakistan. His research interests include antennas and metasurfaces.

• • •